

# Hydrogen-Bonding Interactions in a Single-Component Molecular Conductor: a Hydroxyethyl-Substituted Radical Gold Dithiolene Complex

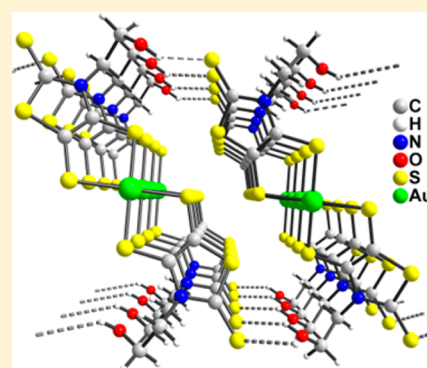
Yann Le Gal,<sup>†</sup> Thierry Roisnel,<sup>†</sup> Pascale Auban-Senzier,<sup>‡</sup> Thierry Guizouarn,<sup>†</sup> and Dominique Lorcy<sup>\*,†</sup>

<sup>†</sup>Institut des Sciences Chimiques de Rennes, UMR 6226 CNRS, Université de Rennes 1, Campus de Beaulieu, Bât 10A, 35042 Rennes Cedex, France

<sup>‡</sup>Laboratoire de Physique des solides UMR 8502 CNRS, Université de Paris-Sud, Bat 510, 91405 Orsay Cedex, France

## Supporting Information

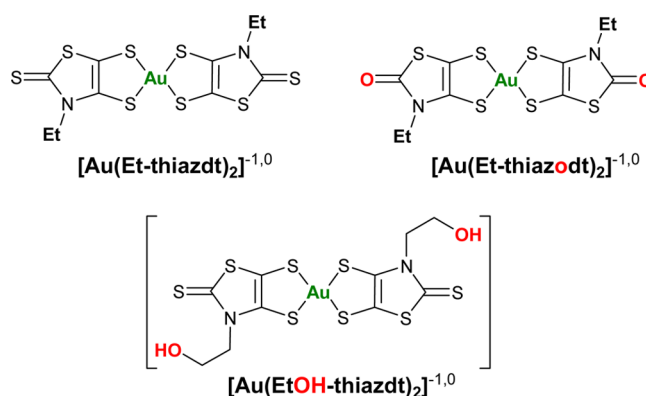
**ABSTRACT:** The anionic hydroxyethyl-substituted gold dithiolene complex  $[\text{NEt}_4][\text{Au}(\text{EtOH-thiazdt})_2]$  is synthesized and further oxidized to the neutral radical species  $[\text{Au}(\text{EtOH-thiazdt})_2]^{\bullet}$  through electrocrystallization. Single-crystal X-ray diffraction studies highlight the existence of the two cis and trans isomers for the monoanionic complex, with involvement of the hydroxy group in intermolecular  $\text{O}-\text{H}\cdots\text{S}$  hydrogen-bonding interactions. The neutral radical complex,  $[\text{Au}(\text{EtOH-thiazdt})_2]^{\bullet}$ , is isostructural with its known ethyl analogue, namely,  $[\text{Au}(\text{Et-thiazdt})_2]^{\bullet}$ . It exhibits a semiconducting behavior ( $\sigma_{\text{RT}} = 0.05\text{--}0.07 \text{ S cm}^{-1}$ ) at room temperature and ambient pressure with an activation energy of 0.14 eV. Comparison of the crystal structures and transport and magnetic properties with those of the prototypical  $[\text{Au}(\text{Et-thiazdt})_2]^{\bullet}$  single-component conductor shows that the replacement of ethyl by a slightly bulkier hydroxyethyl substituent affects only weakly the overlap interactions, complemented here by added  $\text{O}-\text{H}\cdots\text{S}$  hydrogen-bonding interactions.



## INTRODUCTION

For more than 3 decades, bis(1,2-dithiolene) complexes of transition metals have received a lot of attention as building blocks for the elaboration of molecular conductors.<sup>1–3</sup> On this matter, a wide panel of structures have been reported exhibiting in general square-planar geometry and, because of the noninnocent character of the ligands,<sup>4</sup> different redox states involving by stage one electron transfer. Most of these conducting materials are found in mixed-valence salts, which are multicomponent molecular conductors, because they include counterions in their formula. Less investigated are the single-component molecular conductors based on bis(1,2-dithiolene) ligands. These are all neutral complexes and can be divided into two groups: those reported by Kobayashi et al. where various metals ( $M = \text{Ni}, \text{Co}, \text{Cu}, \text{Pd}, \text{and Au}$ ) are coordinated by two tetrathiafulvalene dithiolate ligands<sup>5,6</sup> and the other category in which all gold complexes are surrounded by two electron-rich dithiolene ligands.<sup>7–10</sup> The latter are easily generated from oxidation of the monoanionic species  $[\text{Au}(\text{dithiolene})_2]^-$ . Along these lines, we have recently reported a single-component conductor based on a neutral radical gold dithiolene complex (Chart 1), namely,  $[\text{Au}(\text{Et-thiazdt})_2]^{\bullet}$  (Et-thiazdt = *N*-ethyl-1,3-thiazoline-2-thione-4,5-dithiolate), which adopts a layered structure. Furthermore, this novel type of Mott insulator becomes metallic under an applied pressure of 1.3 GPa.<sup>11</sup> We have also demonstrated that, through small modifications of the dithiolate ligand, it is also possible to

Chart 1



impact the conducting properties (and their pressure dependence) by exercising not only a physical pressure but also a chemical pressure.<sup>12</sup> Actually, this was realized by replacing either the exocyclic sulfur atom by an oxygen atom, as in  $[\text{Au}(\text{Et-thiazodt})_2]^{\bullet}$ , or by substituting the coordinated sulfur atoms of the metallacycles for selenium atoms. These compounds were all isostructural, allowing for a useful comparison of their electronic structures, because the chemical

Received: June 19, 2014

Published: August 1, 2014

pressure effects identified then proved indeed highly anisotropic. For example, the introduction of a smaller exocyclic atom (oxygen vs sulfur) in  $[\text{Au}(\text{Et-thiazodt})_2]^+$  led, as expected, to an average unit cell contraction but surprisingly to a strongly decreased conductivity because the large interlayer compression was actually compensated for by a dilatation within the conducting layers.

Herein, we present another modification of the ligand skeleton that consists of replacing the ethyl substituent of the thiazole ring by other substituents, in order to test the robustness of the prototype structure  $[\text{Au}(\text{Et-thiazdt})_2]^+$  to other structural modifications, as well as their anisotropy. The hydroxyethyl group was first chosen because it adds only *one* extra atom to the ethyl group and also because it opens attractive possibilities for intra- and/or intermolecular hydrogen-bonding interactions, as was already investigated, for example, in organic metals based on mixed-valence cation-radical salts.<sup>13</sup>

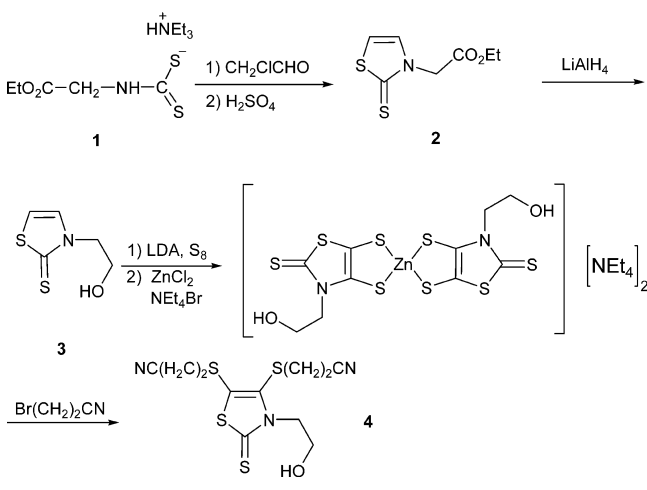
We describe here the synthesis and properties of the anionic precursor  $[\text{Au}(\text{EtOH-thiazdt})_2]^-$ , together with the structural and conducting properties of the desired neutral radical  $[\text{Au}(\text{EtOH-thiazdt})_2]^{\bullet}$ , while comparison with the reported ethyl-substituted  $[\text{Au}(\text{Et-thiazdt})_2]$  and  $[\text{Au}(\text{Et-thiazodt})_2]^+$  dithiolene complexes provides a rationale for the observed conductive properties.

## RESULTS AND DISCUSSION

The synthesis of the anionic gold complex is realized in two stages: first synthesis of the cyanoethyl-protected dithiolene ligand and then synthesis formation of the gold complex through base deprotection of the dithiolate precursor and the addition of a gold(III) salt.

The protected dithiolate molecule **4** was prepared from dithiocarbamate salt **1**,<sup>14</sup> as outlined in Scheme 1 according to a

### Scheme 1. Preparation of the Hydroxyethyl-Substituted Dithiolate Precursor **4**



chemical strategy that we previously used for the synthesis of various thiazoline thiones.<sup>15</sup> Dithiocarbamate salt **1** was reacted with chloroacetaldehyde. Cyclization and dehydration with sulfuric acid led to thiazoline-2-thione **2**. Reduction of the ester group was performed with the use of  $\text{LiAlH}_4$  in dry diethyl ether and afforded the thiazoline thione **3**. Attempts to form the protected dithiolate precursor **4** directly after bismetalation, followed by the addition of sulfur and bromopropionitrile, were

unsuccessful. Therefore, **4** was prepared in two steps: first formation of the dianionic zinc salt occurred through bismetalation of **3** with lithium diisopropylamide (LDA), followed by the addition of  $\text{S}_8$  and the trapping of dithiolate with  $\text{ZnCl}_2$  and  $\text{NEt}_4\text{Br}$  before hydrolysis. Then, in a second step, without isolation of the zinc salt, the addition of bromopropionitrile afforded the thiazoline thione **4** but in rather low yield (15%).<sup>16</sup> Crystals were obtained, and their investigation by X-ray diffraction confirmed the formation of **4**. The compound crystallized in the orthorhombic system, space group  $Pn2_1a$ . The molecular structure is reported in Figure 1

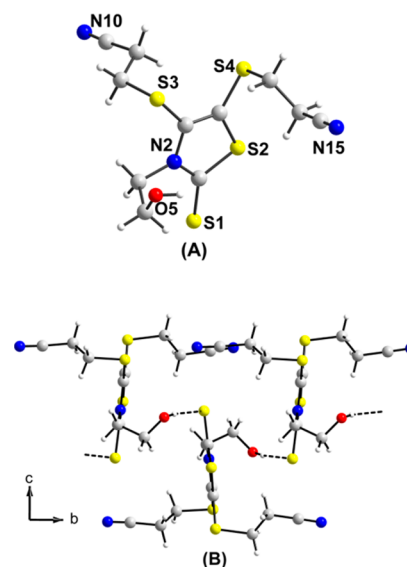


**Figure 1.** (A) Molecular structure of compound **4** showing the atom labeling. (B) View of the O–H...S hydrogen bonding between neighboring molecules along the *b* axis.

**Table 1.** Selected Intramolecular Bond Lengths (Å) in the Dithiolate-Protected Form **4**, Monoanionic *cis*- and *trans*-**5**, and Neutral **6** Dithiolene Complexes

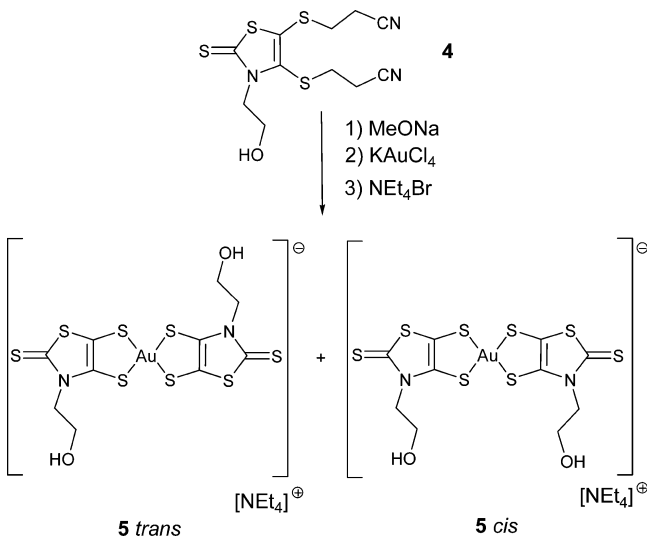
	<i>cis</i> - [Au(EtOH-thiazdt) <sub>2</sub> ] <sup>-</sup> in <b>5</b>	<i>trans</i> - [Au(EtOH-thiazdt) <sub>2</sub> ] <sup>-</sup> in <b>5</b>	<i>trans</i> - [Au(EtOH-thiazdt) <sub>2</sub> ] ( <b>6</b> )
Au–S1	2.326(3)	2.325(4)	2.3197(11)
Au–S11	2.326(3)	2.330(4)	
Au–S2	2.341(3)	2.356(4)	2.3211(12)
Au–S12	2.318(3)	2.361(4)	
S1–C1	1.754(4)	1.779(12)	1.725(5)
S11–C11	1.750(11)	1.769(16)	
S2–C2	1.751(3)	1.747(12)	1.714(5)
S12–C12	1.738(11)	1.764(14)	
C1–C2	1.356(4)	1.294(16)	1.374(7)
C11–C12	1.357(14)	1.35(2)	

(top), and selected bond lengths are collected in Table 1. As expected, the OH group is engaged in hydrogen bonding, but with the sulfur atom of the thione moiety of the thiazole core of a neighboring molecule, with the following characteristics: H...S distance, 2.403(1) Å; O–H...S angle 172.6°. The directionality as well as the interatomic distance, well in the reported range for H...S hydrogen bonds (2.26–2.65 Å),<sup>17</sup> leaves no ambiguity

about the presence of this interaction. It gives rise to a chainlike helical motif along the  $2_1$  screw axis along  $b$  (Figure 1, bottom).

In order to synthesize the monoanionic gold complex  $[\text{NEt}_4][\text{Au}(\text{EtOH-thiazdt})_2]$  (**5**; Scheme 2), sodium methano-

### Scheme 2. Synthesis of the Anionic Gold Complexes



late was added to the thiazoline **4** to generate deprotection of the dithiolate, followed by the addition of  $\text{KAuCl}_4$  and  $\text{NEt}_4\text{Br}$ . The gold complex **5** was isolated as a dark-greenish solid, which was recrystallized in acetonitrile. Two types of crystals were obtained simultaneously, both of them with a stick form but with a different color, one darker than the other. X-ray diffraction studies were carried out on both types. Even if the quality of the darkest crystals is poor and thus the corresponding crystal structure resolution, X-ray diffraction analyses of both revealed that the two isomers were obtained (Scheme 2 and Figure 2). Indeed, because of the dissymmetrical character of the dithiolate ligand, this complex is susceptible to existing in two configurations, the trans and cis ones.

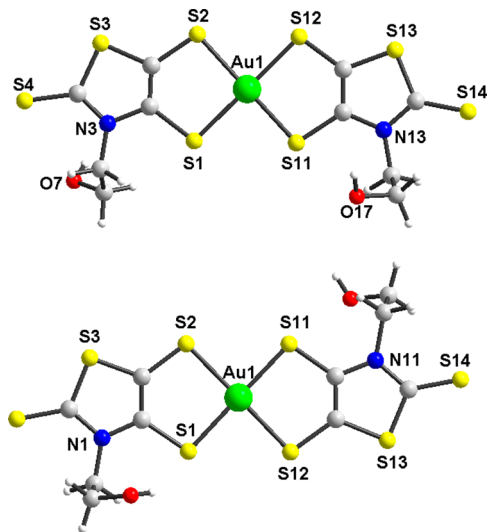


**Figure 2.** Molecular views of the  $\text{cis-}[\text{Au}(\text{EtOH-thiazdt})_2]^-$  complex (top) and the  $\text{trans-}[\text{Au}(\text{EtOH-thiazdt})_2]^-$  complex (bottom) in **5**.

The trans isomer **5** crystallizes in the monoclinic system, space group  $C2/c$ , and the cis isomer **5** crystallizes in the triclinic system, space group  $P\bar{1}$ . Both isomers exhibit a square-planar geometry around the gold atom and a planar skeleton, apart from the hydroxyethyl groups hanging on both sides. Intramolecular bond lengths are collected in Table 1. Due to the dissymmetry of the dithiolene ligand and to the differences in the bond lengths on the side of the nitrogen and the sulfur atom of the thiazole ring, the cis isomer adopts an arc-shaped geometry while the trans isomer is linear. Moreover, for both isomers, we can also notice, as observed above in the structure of **4**, the presence of  $\text{O-H}\cdots\text{S}$  hydrogen bonding between the hydroxy and thione of a thiazole core (Figure 3). Within the

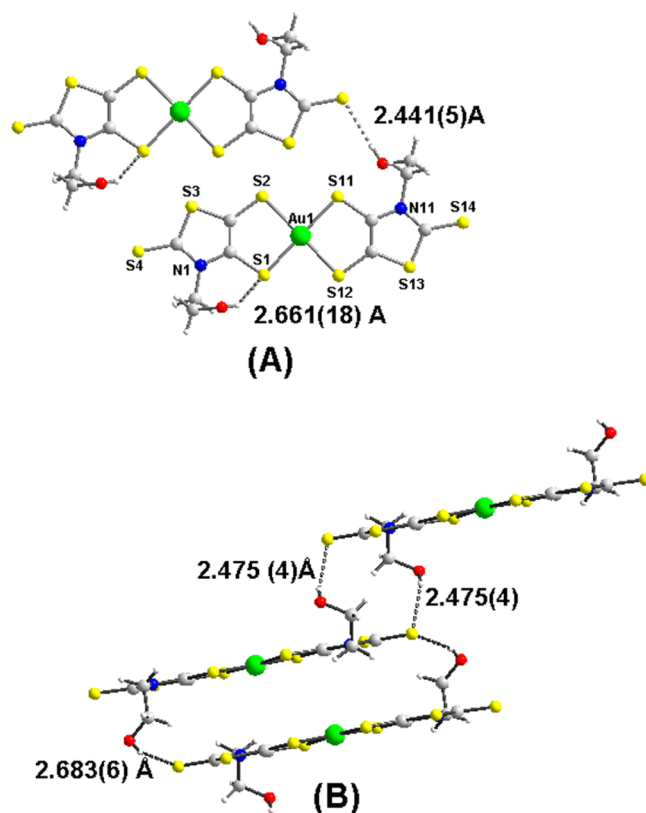


**Figure 3.** View of the  $\text{O-H}\cdots\text{S}$  hydrogen bonding in  $\text{trans-}[\text{Au}(\text{EtOH-thiazdt})_2]^-$  (A) and  $\text{cis-}[\text{Au}(\text{EtOH-thiazdt})_2]^-$  (B).

trans isomer, an intramolecular  $\text{H}\cdots\text{S}$  distance of  $2.661(18)$  Å is observed, leading to a seven-membered ring, together with an intermolecular  $\text{H}\cdots\text{S}$  distance of  $2.441(5)$  Å between two neighboring complexes. On the contrary, for the cis isomer, only intermolecular  $\text{O-H}\cdots\text{S}$  hydrogen-bonding interactions are observed.

Oxidation of **5** has been realized by electrocrystallization upon application of a current intensity of  $0.2 \mu\text{A}$  in the presence of  $\text{NBu}_4\text{PF}_6$  as the supporting electrolyte in  $\text{CH}_2\text{Cl}_2$ . Using these conditions, small crystals, suitable for an X-ray diffraction study, were collected at the anode. The neutral complex  $[\text{Au}(\text{EtOH-thiazdt})_2]$  (**6**) crystallizes in the monoclinic system, space group  $P2_1/a$ . It is isostructural with the previously reported examples of neutral gold dithiolene complexes belonging to the same family with a thiazole backbone, such as  $[\text{Au}(\text{Et-thiazdt})_2]$  and  $[\text{Au}(\text{Et-thiazodt})_2]$  (Chart 1). Thus,  $[\text{Au}(\text{EtOH-thiazdt})_2]$ , which is under the trans configuration with a planar skeleton, adopts the same

organization in the solid state (Figure 4): (i) it forms uniform stacks along  $b$  with a lateral slip between neighboring

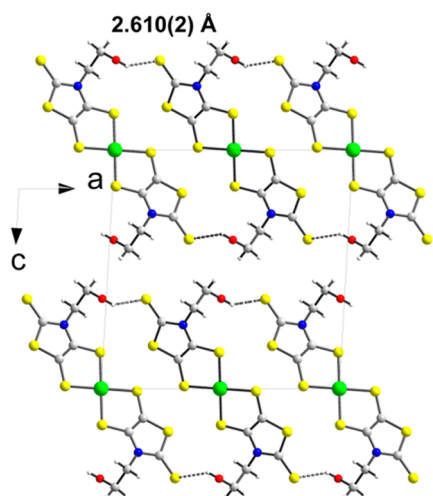


**Figure 4.** Projection view along  $b$  of the unit cell of  $[\text{Au}(\text{EtOH-thiazdt})_2]$  showing the intermolecular  $\text{O-H}\cdots\text{S}$  hydrogen bonding between neighboring complexes.

complexes, and the shortest  $\text{S}\cdots\text{S}$  contact amounts to  $3.866(4)$  Å; (ii) the complexes interact laterally along  $a$  with several  $\text{S}\cdots\text{S}$  contacts (Figure 5). As observed for the *cis* and

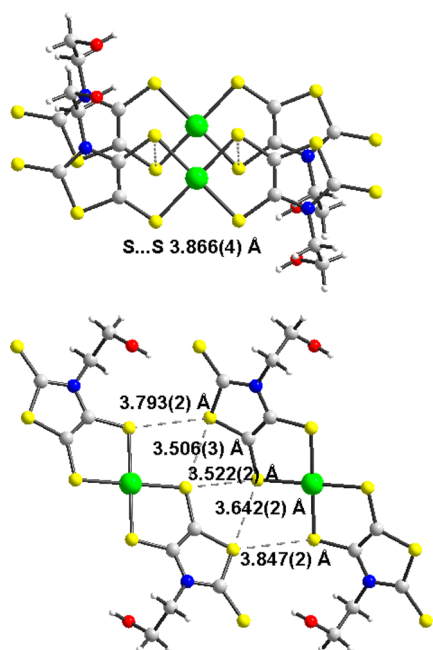


**Figure 5.** View of the short  $\text{S}\cdots\text{S}$  contacts along the stacking axis  $b$  (top) and between the stacks along  $a$  (bottom).

trans monoanionic complexes, intermolecular  $\text{O-H}\cdots\text{S}$  hydrogen bonding is also observed, with a  $\text{H}\cdots\text{O}$  distance being equal to  $2.610(2)$  Å, between neighboring complexes along  $a$ .

Because of the very small crystal size, resistivity measurements were carried out at two points on a polycrystalline sample. The room temperature conductivity at ambient pressure is estimated to  $0.05\text{--}0.07$   $\text{S cm}^{-1}$ , and upon cooling, semiconducting behavior is observed with an activation energy of  $0.14$  eV (Figure 6). It is difficult to compare this result with

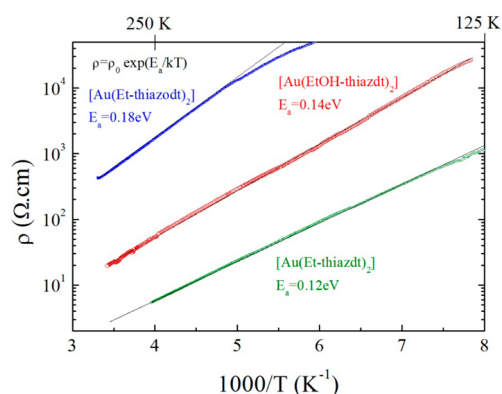


**Figure 6.** (a) Resistivity data of  $[\text{Au}(\text{EtOH-thiazdt})_2]$  (red points) compared to  $[\text{Au}(\text{Et-thiazdt})_2]$  (green points) and  $[\text{Au}(\text{Et-thiazodt})_2]$  (blue points) plotted as  $\rho$  versus the inverse temperature. The black lines are linear fit to the data, giving the activation energies  $E_a$ .

previously reported data in the prototype  $[\text{Au}(\text{Et-thiazdt})_2]$ <sup>11</sup> and the other isostructural complex with the outer carbonyl function, that is,  $[\text{Au}(\text{Et-thiazodt})_2]$ ,<sup>12</sup> because in these two cases the conductivity was measured on single crystal at four points aligned along the long axis of the needles (corresponding to the stacking axis). Nevertheless, as shown in Figure 6, the conductivity is lower and the activation energy is higher than the values found for  $[\text{Au}(\text{Et-thiazdt})_2]$ , while they are respectively higher and lower than the values found for  $[\text{Au}(\text{Et-thiazodt})_2]$ .

Susceptibility data are shown in Figure 7, together with those reported for the two other isostructural dithiolenes complexes,

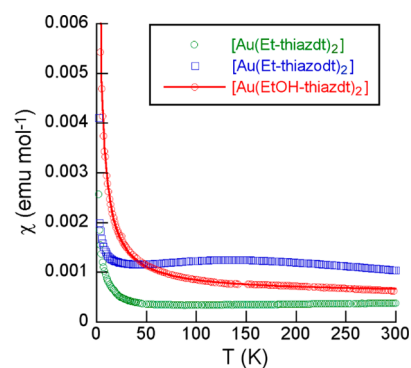


**Figure 7.** Temperature dependence of the magnetic susceptibility of  $[\text{Au}(\text{EtOH-thiazdt})_2]$ , together with those of reference complexes.

that is,  $[\text{Au}(\text{Et-thiazdt})_2]$  and  $[\text{Au}(\text{Et-thiazodt})_2]$ . The compound is only weakly magnetic, with a magnetic susceptibility well fitted as a Curie–Weiss law,  $\chi = \chi_0 + C/T$ , with a  $C$  value corresponding to 2.82% of the  $S = 1/2$  species and a  $\chi_0$  value of  $0.57 \times 10^{-3}$   $\text{emu mol}^{-1}$ . The  $\chi_0$  value is intermediate with those found for the more conductive  $[\text{Au}(\text{Et-thiazdt})_2]$  ( $\chi_0 = 10^{-4}$   $\text{emu mol}^{-1}$ ) and the less conductive  $[\text{Au}(\text{Et-thiazodt})_2]$  ( $\chi_0 = 10^{-3}$   $\text{emu mol}^{-1}$ ), where the stronger spin localization was visible from the more pronounced uniform spin-chain behavior. In conclusion, both transport and magnetic measurements indicate that the hydroxyethyl derivative  $[\text{Au}(\text{EtOH-thiazdt})_2]$ , despite a larger unit cell volume, appears to be intermediate between the two other dithiolenes complexes,  $[\text{Au}(\text{Et-thiazdt})_2]$  and  $[\text{Au}(\text{Et-thiazodt})_2]$ .



A close look at the unit cell dimensions of  $[\text{Au}(\text{EtOH-thiazdt})_2]$  compared with those of  $[\text{Au}(\text{Et-thiazdt})_2]$  and  $[\text{Au}(\text{Et-thiazodt})_2]$  is indicative of the influence of the hydroxyethyl group (Table 2). It can be observed that the

**Table 2. Comparison of the Unit Cell Data and  $\beta_{\text{HOMO-HOMO}}$  Interaction Energies (Intrastacking and Interstacking) in the Three Complexes<sup>a</sup>**

	$[\text{Au}(\text{Et-thiazdt})_2]$	$[\text{Au}(\text{Et-thiazodt})_2]$	$[\text{Au}(\text{EtOH-thiazdt})_2]$
<i>T</i> (K)	100	150	150
<i>a</i> (Å)	14.060	14.135 (+0.53%)	14.2789 (+1.56%)
<i>b</i> (Å)	4.0593	4.1370 (+1.91%)	4.1546 (+2.34%)
<i>c</i> (Å)	14.259	13.460 (−5.60%)	14.3699 (+0.78%)
<i>V</i> (Å <sup>3</sup> )	812.3	781.0 (−3.85%)	851.07 (+4.77%)
$\beta_{\text{intra}}$ (eV)	0.226	0.187 (−17%)	0.192 (−15%)
$\beta_{\text{inter}}$ (eV)	0.049	0.056	0.042

<sup>a</sup>In parentheses are given the length evolution relative to the  $[\text{Au}(\text{Et-thiazdt})_2]$  reference complex.

presence of the extra oxygen induces a unit cell expansion along the three directions of space, which mainly affects the *b* stacking axis and then the interstacking *a* axis. This contrasts with the anisotropic cell modifications found for  $[\text{Au}(\text{Et-thiazodt})_2]$ , where the large unit cell volume decrease was actually concentrated between the conducting slabs (along the *c* direction), along with an associated slab expansion (along *a* and *b*). This anisotropic chemical pressure effect was responsible for the decreased overlap interactions within the stacks, as illustrated by the lowered  $\beta_{\text{intra}}$  value for  $[\text{Au}(\text{Et-thiazodt})_2]$ . Here, the larger hydroxyethyl group indeed pushes the radicals apart from each other within the layers, as in  $[\text{Au}(\text{Et-thiazodt})_2]$ , but to a lesser extent. This provides a rationale for the intermediate room temperature conductivity and activation energy found for the title compound compared with the two other members of the series.

Extended Hückel (EH) band structure calculations were performed on the three complexes in order to evaluate these evolutions within the series (Figure 8). These calculations predict a metallic character for the three compounds, with a Fermi level cutting two or even three bands, in contradiction with the actual semiconducting behavior. However, they already demonstrate that the semiconducting behavior does not have a structural origin (dimerization, Peierls transition, etc.). Earlier ab initio calculations have shown indeed that electron–electron repulsions are able to open a Mott–Hubbard gap in these systems, providing a rationale for the observed Mott insulator character.<sup>11,12</sup> The reference complex  $[\text{Au}(\text{Et-thiazdt})_2]$  was found with a very small Mott–Hubbard gap and was sensitive to the pressure, becoming metallic above 1.3 GPa. The less conductive oxygen-substituted derivative  $[\text{Au}(\text{Et-thiazodt})_2]$  was predicted with a much larger Mott–Hubbard gap, in accordance with a larger activation energy. The comparison of the EH band structures for the three complexes confirms indeed the intermediate character of the hydroxyethyl-substituted complex  $[\text{Au}(\text{EtOH-thiazdt})_2]$  deduced from the transport and magnetic properties. It is particularly visible at the  $\Gamma$  point of the Brillouin zone (Figure 8), where the two lower bands are well separated from the two upper ones in  $[\text{Au}(\text{Et-thiazodt})_2]$ , as in  $[\text{Au}(\text{EtOH-thiazdt})_2]$ . On the other hand, in the most conducting  $[\text{Au}(\text{Et-thiazdt})_2]$  complex, they rise in energy to a point where they actually cut the Fermi level,

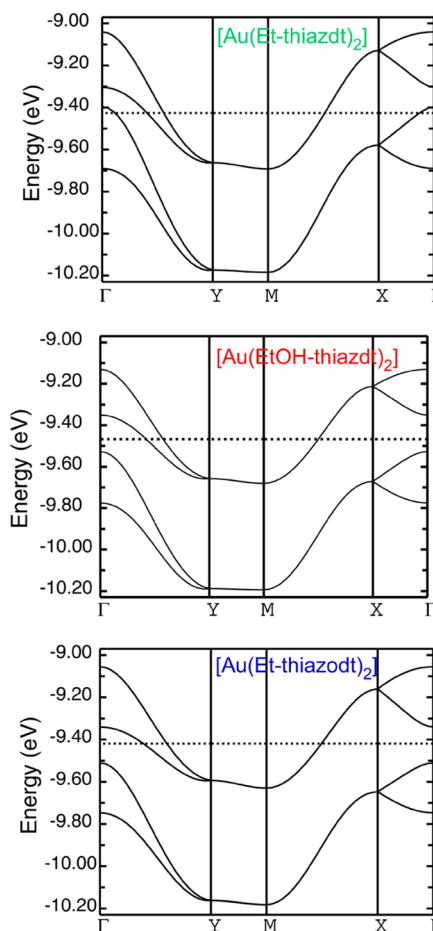


**Figure 8.** Calculated (EH) band structures for the three complexes  $[\text{Au}(\text{Et-thiazdt})_2]$ ,  $[\text{Au}(\text{EtOH-thiazdt})_2]$ , and  $[\text{Au}(\text{Et-thiazodt})_2]$ , with notable differences at the  $\Gamma$  point.

allowing for stabilization of the metallic state in this last system, at least under moderate pressures.

In conclusion, these neutral radical gold complexes provide an extensive series of single-component conductors whose solid-state organization, and associated electronic properties, proved highly sensitive to minute structural modifications. Already illustrated earlier with chalcogen atom substitution strategies (oxygen vs sulfur and sulfur vs selenium), it is further emphasized here with the addition of only one extra oxygen atom. The robustness of this layered structure is also illustrated here by the isostructural character with the ethyl-substituted complexes and the setting of intra- and intermolecular O–H⋯S hydrogen bonds rather than the possibly stronger O–H⋯O hydrogen bonds. We are currently investigating how slightly smaller or larger substituents than the ethyl one could further affect this prototype structure of single-component conductors.

## ■ EXPERIMENTAL SECTION

All commercial reagents were used as purchased. The dithiocarbamate salt **1** was synthesized according to a literature procedure.<sup>14</sup> All air-sensitive reactions were carried out under an argon atmosphere. The solvents were purified and dried by standard methods. Column chromatography was performed using Merck silica gel 60 (70–260 mesh). <sup>1</sup>H and <sup>13</sup>C NMR spectra were recorded on a Bruker AV300III spectrometer. Chemical shifts are quoted in parts per million (ppm) referenced to tetramethylsilane. Melting points were measured on a Kofler hot-stage apparatus and are uncorrected. Mass spectra were recorded with a Waters Q-ToF 2 instrument by the Centre Régional de

Table 3. Crystallographic Data

	4	<i>cis</i> -5	<i>trans</i> -5	[Au(EtOH-thiazdt) <sub>2</sub> ]
formula	C <sub>11</sub> H <sub>13</sub> N <sub>3</sub> O <sub>3</sub> S <sub>4</sub>	C <sub>18</sub> H <sub>30</sub> AuN <sub>3</sub> O <sub>2</sub> S <sub>8</sub>	C <sub>18</sub> H <sub>30</sub> AuN <sub>3</sub> O <sub>2</sub> S <sub>8</sub>	C <sub>10</sub> H <sub>10</sub> AuN <sub>2</sub> O <sub>2</sub> S <sub>8</sub>
fw (g mol <sup>-1</sup> )	331.48	773.9	773.9	643.65
cryst syst	orthorhombic	triclinic	monoclinic	monoclinic
space group	<i>Ph</i> 2 <sub>1</sub> <i>a</i>	<i>P</i> $\bar{1}$	<i>C</i> 2/ <i>c</i>	<i>P</i> 2 <sub>1</sub> / <i>a</i>
<i>a</i> (Å)	7.2442(7)	8.3506	37.486(12)	14.2789(9)
<i>b</i> (Å)	8.6309(11)	11.9220(6)	7.659(3)	4.1546(3)
<i>c</i> (Å)	23.855(3)	15.0121(7)	19.413(7)	14.3699(8)
$\alpha$ (deg)	90	103.813(2)	90	90
$\beta$ (deg)	90	103.408(2)	97.248(17)	93.286(3)
$\gamma$ (deg)	90	103.106(2)	90	90
<i>V</i> (Å <sup>3</sup> )	1491.51(30)	1347.33(10)	5529(3)	851.07(9)
<i>T</i> (K)	150(2)	150(2)	150(2)	150(2)
<i>Z</i>	4	2	8	2
<i>D</i> <sub>calc</sub> (g cm <sup>-3</sup> )	1.476	1.908	1.859	2.512
$\mu$ (mm <sup>-1</sup> )	0.631	6.102	5.948	9.631
total no. of reflns	6636	14414	17193	10798
unique reflns ( <i>R</i> <sub>int</sub> )	2477 (0.0463)	6079 (0.0629)	6178 (0.136)	1959 (0.0476)
unique reflns [ <i>I</i> > 2 $\sigma$ ( <i>I</i> )]	2327	3991	3412	1617
<i>R</i> <sub>1</sub> , <i>wR</i> <sub>2</sub>	0.0427, 0.1046	0.0546, 0.1149	0.0835, 0.1881	0.0255, 0.0556
<i>R</i> <sub>1</sub> , <i>wR</i> <sub>2</sub> (all data)	0.0459, 0.1074	0.1048, 0.1559	0.1576, 0.2345	0.035, 0.0599
GOF	1.028	1.039	0.978	1.09

Mesures Physiques de l'Ouest, Rennes, France. Elemental analysis was performed at the Centre Régional de Mesures Physiques de l'Ouest, Rennes, France.

**Ethyl (2-Thioxo-1,3-thiazol-3-yl)acetate (2).** To a suspension of the dithiocarbamate salt **1** (20.60 g, 73.6 mmol) in acetonitrile (250 mL) was added chloroacetaldehyde (50% solution in water, 9.34 mL, 73.6 mmol). The mixture was stirred for 24 h at room temperature under nitrogen. The volume was reduced to approximately one-fifth in vacuo, and the solution was slowly added to a flask containing 20 mL of H<sub>2</sub>SO<sub>4</sub> at 0 °C. The mixture was stirred for 15 min at 0 °C, hydrolyzed with 100 mL of water, and extracted with CH<sub>2</sub>Cl<sub>2</sub> (3 × 80 mL). The organic phase was washed with water (3 × 50 mL) and dried over MgSO<sub>4</sub>. The concentrated solution was purified by chromatography on silica gel using CH<sub>2</sub>Cl<sub>2</sub> as the eluant to afford **1** as a pale-brown oil. Yield: 46%. <sup>1</sup>H NMR (300 MHz, CDCl<sub>3</sub>):  $\delta$  1.27 (t, 3H, CH<sub>2</sub>CH<sub>3</sub>, *J* = 7.1 Hz), 4.22 (q, 3H, CH<sub>2</sub>CH<sub>3</sub>, *J* = 7.1 Hz), 4.92 (s, 2H, NCH<sub>2</sub>), 6.62 (d, 1H, CH, *J* = 4.6 Hz), 7.08 (d, 1H, CH, *J* = 4.6 Hz). <sup>13</sup>C NMR (75 MHz, CDCl<sub>3</sub>):  $\delta$  14.0 (CH<sub>3</sub>), 50.0 (CH<sub>2</sub>), 62.0 (CH<sub>2</sub>), 110.6 (C=C), 131.5 (C=C), 166.3 (CO<sub>2</sub>), 188.7 (C=S). HRMS (ESI). Calcd for C<sub>7</sub>H<sub>9</sub>NO<sub>2</sub>NaS<sub>2</sub> [M<sup>+</sup>Na]<sup>+</sup>: *m/z* 225.9972. Found: *m/z* 225.9971. Anal. Calcd for C<sub>7</sub>H<sub>9</sub>NO<sub>2</sub>S<sub>2</sub>: C, 41.36; H, 4.46; N, 6.89; S, 31.55. Found: C, 40.89; H, 4.45; N, 6.75; S, 31.56.

**Preparation of 3-(2-Hydroxyethyl)-1,3-thiazoline-2-thione (3).** Into a cooled solution (0 °C) of LiAlH<sub>4</sub> (4 M solution in diethyl ether, 4.90 mL, 19.7 mmol) in 50 mL of dry THF under nitrogen was dropped a solution of thiazoline **2** (2.0 g, 9.85 mmol) in 15 mL of dry THF. The mixture was stirred for 30 min at 0 °C and 30 min further at room temperature. The reaction solution was cooled again to 0 °C, and a mixture of 50 mL of water and 50 mL of THF was added slowly. Then the reaction mixture was acidified by 4 M HCl (100 mL) and extracted with ethyl acetate (3 × 60 mL). The organic phase was washed with brine (3 × 60 mL) and water (3 × 60 mL) and dried over Na<sub>2</sub>SO<sub>4</sub>. The concentrated solution was purified by chromatography on silica gel using CH<sub>2</sub>Cl<sub>2</sub> as the eluant to afford **3** as a pale-brown powder. Yield: 65%. Mp: 56 °C. <sup>1</sup>H NMR (300 MHz, CDCl<sub>3</sub>):  $\delta$  2.71 (s, 1H, OH), 3.97 (t, 2H, CH<sub>2</sub>CH<sub>2</sub>, *J* = 5.1 Hz), 4.33 (t, 2H, CH<sub>2</sub>CH<sub>2</sub>, *J* = 5.1 Hz), 6.60 (d, 1H, CH, *J* = 4.8 Hz), 7.21 (d, 1H, CH, *J* = 4.8 Hz). <sup>13</sup>C NMR (75 MHz, CDCl<sub>3</sub>):  $\delta$  51.9 (CH<sub>2</sub>), 60.1 (CH<sub>2</sub>), 110.7 (C=C), 132.9 (C=C), 187.5 (C=S). HRMS (ESI). Calcd for C<sub>5</sub>H<sub>7</sub>NONaS<sub>2</sub> [M<sup>+</sup>Na]<sup>+</sup>: *m/z* 183.9866. Found: *m/z* 183.9854. Anal. Calcd for C<sub>5</sub>H<sub>7</sub>NONOS<sub>2</sub>: C, 37.24; H, 4.38; N, 8.69. Found: C, 37.42; H, 4.27; N, 8.37.

**3,3'-[3-(2-Hydroxyethyl)-2-thioxo-2,3-dihydro-1,3-thiazole-4,5-diyl]bis(thio)dipropanenitrile (4).** To a -10 °C cooled solution of thiazoline **3** (1 g, 6.2 mmol) in 40 mL of dry THF under nitrogen was added a solution of LDA prepared from diisopropylamine (2.2 mL, 15.5 mmol) and 1.6 M *n*-BuLi in hexane (9.7 mL, 15.5 mmol) in 25 mL of dry THF. After stirring for 30 min at -10 °C, sulfur S<sub>8</sub> (300 mg, 9.3 mmol) was added, and the solution was stirred for an additional 30 min. A solution of LDA [diisopropylamine (1.8 mL, 12.4 mmol) and 1.6 M *n*-BuLi in hexane (7.8 mL, 12.4 mmol)] in 20 mL of dry THF was then added. The mixture was stirred for 3 h, and S<sub>8</sub> (400 mg, 12.4 mmol) was added. After 30 min, ZnCl<sub>2</sub> (423 mg, 3.1 mmol) and NEt<sub>4</sub>Br (1.3 g, 6.2 mmol) were added. The reaction mixture was stirred overnight, and 10 mL of water was added. The solvents were evaporated in vacuo. The crude product was dissolved in 100 mL of acetonitrile, and bromopropionitrile (0.90 mL, 10.9 mmol) was added. The reaction mixture is heated to reflux for 12 h, and the solvent was removed in vacuo. The concentrated solution was purified by chromatography on silica gel using the mixture CH<sub>2</sub>Cl<sub>2</sub>/Et<sub>2</sub>O (4:1) as the eluant to eliminate the secondary products and then ethyl acetate as the eluant to afford compound **4**. Recrystallization in CH<sub>2</sub>Cl<sub>2</sub>/Et<sub>2</sub>O gave pale-brown crystals. Yield: 15%. Mp: 98 °C. <sup>1</sup>H NMR (300 MHz, CDCl<sub>3</sub>):  $\delta$  2.10 (t, 1H, OH, *J* = 5.7 Hz), 2.74 (m, 4H, CH<sub>2</sub>CN), 3.11 (t, 2H, SCH<sub>2</sub>, *J* = 6.9 Hz), 3.24 (t, 2H, SCH<sub>2</sub>, *J* = 6.9 Hz), 3.85 (m, 2H, CH<sub>2</sub>OH), 4.51 (t, 2H, NCH<sub>2</sub>, *J* = 5.4 Hz). <sup>13</sup>C NMR (75 MHz, CDCl<sub>3</sub>):  $\delta$  19.1, 32.4, 32.7, 52.1, 58.6, 118.2, 119.3, 119.4, 126.2, 138.8, 188.9. Anal. Calcd for C<sub>11</sub>H<sub>13</sub>N<sub>3</sub>O<sub>3</sub>S<sub>4</sub>: C, 38.96; H, 3.95; N, 12.68. Found: C, 40.34; H, 3.84; N, 12.54. HRMS (ESI). Calcd for C<sub>11</sub>H<sub>13</sub>N<sub>3</sub>O<sub>3</sub>S<sub>4</sub> [M<sup>+</sup>Na]<sup>+</sup>: *m/z* 353.9839. Found: *m/z* 353.9841.

**[NEt<sub>4</sub>][Au(EtOH-thiazdt)<sub>2</sub>] (5).** To a dry two-necked flask containing thiazoline-2-thione **4** (140 mg, 0.42 mmol) was added a solution of NaOMe (3.4 mmol) in dry MeOH (prepared from 77 mg of Na in 10 mL of dry MeOH). The solution was stirred for 1 h, and a solution of KAuC<sub>4</sub> (96 mg, 0.25 mmol) in 15 mL of dry MeOH was added. The reaction mixture was stirred for 12 h at room temperature, and NEt<sub>4</sub>Br (133 mg, 0.63 mmol) was added. The mixture was stirred at room temperature for 24 h, and the precipitate was filtered and recrystallized in Me<sub>3</sub>CN to afford **4** as dark crystals. Yield: 25%. Mp: 194 °C. <sup>1</sup>H NMR (300 MHz, (CD<sub>3</sub>)<sub>2</sub>SO):  $\delta$  1.15 (m, 12H, CH<sub>3</sub>), 3.18 (q, 8H, CH<sub>2</sub>, *J* = 7.1 Hz), 3.62 (m, 4H, CH<sub>2</sub>OH), 4.08 (t, NCH<sub>2</sub>, *J* = 7.1 Hz), 5.03 (t, OH, *J* = 5.7 Hz). <sup>13</sup>C NMR (75 MHz, (CD<sub>3</sub>)<sub>2</sub>SO):  $\delta$  7.0, 49.2, 51.3, 51.25, 51.29, 51.33, 56.7, 110.0, 110.1, 131.9, 132.1, 191.0. Anal. Calcd for C<sub>18</sub>H<sub>30</sub>N<sub>3</sub>O<sub>2</sub>S<sub>8</sub>Au: C, 27.93; H, 3.91; N, 5.43.

Found: C, 28.56; H, 3.89; N, 5.48. HRMS (ESI). Calcd for  $[2C^+, A^-]^+$   $C_{26}H_{50}N_4O_2S_8Au$ :  $m/z$  903.1359. Found:  $m/z$  903.1363.

**Electrocrystallization.** Crystals of **6** were prepared electrochemically using a standard H-shaped cell (12 mL) with platinum electrodes. A dichloromethane solution of **5** (10 mg) was placed in the anodic compartment and  $nBu_4NPF_6$  (100 mg) in both compartments. Black needle crystals of  $[Au(EtOH-thiazdt)_2]$  suitable for X-ray diffraction studies were obtained on the anode upon application of a constant current of 0.2  $\mu A$  for 10 days.

**Crystallography.** Single-crystal diffraction data were collected on an APEXII, Bruker-AXS diffractometer, with Mo  $K\alpha$  radiation ( $\lambda = 0.71073 \text{ \AA}$ ) for all compounds. The structures were solved by direct methods using the SIR97 program<sup>18</sup> and then refined with full-matrix least-squares methods based on  $F^2$  (SHELXL-97)<sup>19</sup> with the aid of the WINGX program.<sup>20</sup> All non-hydrogen atoms were refined with anisotropic atomic displacement parameters. Hydrogen atoms were finally included in their calculated positions. Details of the final refinements are given in Table 3.

**Resistivity Measurements.** The resistivity measurements were performed at two points on a multicomponent crystalline sample of  $[Au(EtOH-thiazdt)_2]$ . A constant voltage of 5 mV was applied to the sample, and the current was measured during cooling using a Keithley 6487 direct-current voltage source/picoammeter. Variable temperature between 10 and 300 K was provided by a cryocooler.

**Band Structure Calculations.** The tight-binding band structure calculations and  $\beta_{HOMO-HOMO}$  interaction energies were based on the effective one-electron Hamiltonian of the EH method,<sup>21</sup> as implemented in the Caesar 1.0 chain of programs.<sup>22</sup> The off-diagonal matrix elements of the Hamiltonian were calculated according to the modified Wolfsberg–Helmholz formula.<sup>23</sup> All valence electrons were explicitly taken into account in the calculations, and the basis set consisted of double- $\zeta$  Slater-type orbitals for all atoms except hydrogen and single- $\zeta$  Slater-type orbitals for hydrogen atoms.

## ■ ASSOCIATED CONTENT

### 📄 Supporting Information

X-ray crystallographic files in CIF format. This material is available free of charge via the Internet at <http://pubs.acs.org>.

## ■ AUTHOR INFORMATION

### Corresponding Author

\*E-mail: [Dominique.lorcy@univ-rennes1.fr](mailto:Dominique.lorcy@univ-rennes1.fr).

### Notes

The authors declare no competing financial interest.

## ■ ACKNOWLEDGMENTS

We thank the ANR (France) for financial support through Project 12-BS07-0032. The authors thank Dr. M. Fourmigué for band structure calculations and fruitful discussions.

## ■ REFERENCES

- (1) (a) Kato, R. *Bull. Chem. Soc. Jpn.* **2014**, *87*, 355–374. (b) Kato, R. *Chem. Rev.* **2004**, *104*, 5319–5346.
- (2) Robertson, N.; Cronin, L. *Coord. Chem. Rev.* **2002**, *227*, 93–127.
- (3) Canadell, E. *Coord. Chem. Rev.* **1999**, *185–186*, 629–651. Pullen, A. E.; Olk, R.-M. *Coord. Chem. Rev.* **1999**, *188*, 211–262. Cassoux, P.; Valade, L.; Kobayashi, H.; Kobayashi, A.; Clark, R. A.; Underhill, A. E. *Coord. Chem. Rev.* **1991**, *110*, 115–160.
- (4) Eisenberg, R.; Gray, H. B. *Inorg. Chem.* **2011**, *50*, 9741–9751.
- (5) Kobayashi, A.; Fujiwara, E.; Kobayashi, H. *Chem. Rev.* **2004**, *104*, 5243–5264.
- (6) (a) Cui, H. B.; Kobayashi, H.; Ishibashi, S.; Sasa, M.; Iwase, F.; Kato, R.; Kobayashi, A. *J. Am. Chem. Soc.* **2014**, *136*, 7619–7622. (b) Zhou, B.; Idobata, Y.; Kobayashi, A.; Cui, H.; Kato, R.; Takagi, R.; Miyagawa, K.; Kanoda, K.; Kobayashi, H. *J. Am. Chem. Soc.* **2012**, *134*, 12724–12731. (c) Okano, Y.; Zhou, B.; Tanaka, H.; Adachi, T.;

Ohishi, Y.; Takata, M.; Aoyagi, S.; Nishibori, E.; Sakata, M.; Kobayashi, A.; Kobayashi, H. *J. Am. Chem. Soc.* **2009**, *131*, 7169–7174.

(7) Schiødt, N. C.; Bjørnholm, T.; Bechgaard, K.; Neumeier, J. J.; Allgeier, C.; Jacobsen, C. S.; Thorup, N. *Phys. Rev. B* **1996**, *53*, 1773–1778.

(8) Belo, D.; Alves, H.; Lopes, E. B.; Duarte, M. T.; Gama, V.; Henriques, R. T.; Almeida, M.; Pérez-Benítez, A.; Rovira, C.; Veciana, J. *Chem.—Eur. J.* **2001**, *7*, 511–519.

(9) Dautel, O. J.; Fourmigué, M.; Canadell, E.; Auban-Senzier, P. *Adv. Funct. Mater.* **2002**, *12*, 693–698.

(10) Oliveira, S.; Afonso, M. L.; Dias, S. I. G.; Santos, I. C.; Henriques, R. T.; Rabaça, S.; Almeida, M. *Eur. J. Inorg. Chem.* **2013**, 3133–3136.

(11) Tenn, N.; Bellec, N.; Jeannin, O.; Piekara-Sady, L.; Auban-Senzier, P.; Iniguez, J.; Canadell, E.; Lorcy, D. *J. Am. Chem. Soc.* **2009**, *131*, 16961–16967.

(12) Yzambart, G.; Bellec, N.; Ghassan, N.; Jeannin, O.; Roisnel, T.; Fourmigué, M.; Auban-Senzier, P.; Íñiguez, J.; Canadell, E.; Lorcy, D. *J. Am. Chem. Soc.* **2012**, *134*, 17138–17148.

(13) (a) Fourmigué, M.; Batail, P. *Chem. Rev.* **2004**, *104*, 5379–5418.

(b) Isono, T.; Kamo, H.; Ueda, A.; Takahashi, K.; Nakao, A.; Kumai, R.; Nakao, H.; Kobayashi, K.; Murakami, Y.; Mori, H. *Nat. Commun.* **2013**, *4*, 1344–1349.

(14) Olivier, C.; Toplak, R.; Guerro, M.; Carlier, R.; Lorcy, D. *C. R. Chimie* **2005**, *8*, 235–242.

(15) (a) Bellec, N.; Lorcy, D.; Robert, A.; Carlier, R.; Tallec, A.; Rimbaud, C.; Ouahab, L.; Clerac, R.; Delhaes, P. *Adv. Mater.* **1997**, *9*, 1052–1056. (b) Bellec, N.; Lorcy, D.; Robert, A. *Synthesis* **1998**, 1442–1446. (c) Bellec, N.; Lorcy, D.; Boubekeur, K.; Carlier, R.; Tallec, A.; Los, Sz.; Pukacki, W.; Trybula, M.; Piekara-Sady, L.; Robert, A. *Chem. Mater.* **1999**, *11*, 3147–3153. (d) Guérin, D.; Carlier, R.; Lorcy, D. *J. Org. Chem.* **2000**, *65*, 6069–6072. (e) Guérin, D.; Carlier, R.; Guerro, M.; Lorcy, D. *Tetrahedron* **2003**, *59*, 5273–5279.

(16) Bssaibes, T.; Guerro, M.; Le Gal, Y.; Sarraf, D.; Bellec, N.; Fourmigué, M.; Barriere, F.; Dorcet, V.; Guizouarn, T.; Roisnel, T.; Lorcy, D. *Inorg. Chem.* **2013**, *52*, 2162–2173.

(17) Steiner, T. *Angew. Chem., Int. Ed.* **2002**, *41*, 48–76.

(18) Altomare, A.; Burla, M. C.; Camalli, M.; Casciarano, G.; Giacovazzo, C.; Guagliardi, A.; Moliterni, A. G. G.; Polidori, G.; Spagna, R. *J. Appl. Crystallogr.* **1999**, *32*, 115–119.

(19) Sheldrick, G. M. *Acta Crystallogr.* **2008**, *A64*, 112–122.

(20) Farrugia, L. J. *J. Appl. Crystallogr.* **1999**, *32*, 837–838.

(21) Whangbo, M.-H.; Hoffmann, R. *J. Am. Chem. Soc.* **1978**, *100*, 6093–6098.

(22) Ren, J.; Liang, W.; Whangbo, M.-H. *Crystal and Electronic Structure Analysis Using CAESAR; PrimeColor Software, Inc.:* Cary, NC, 1998.

(23) Ammeter, J.; Bürgi, H.-B.; Thibeault, J.; Hoffmann, R. *J. Am. Chem. Soc.* **1978**, *100*, 3686–3692.